

Cite this: *Catal. Sci. Technol.*, 2019, 9, 6222Received 29th June 2019,  
Accepted 7th October 2019

DOI: 10.1039/c9cy01290g

rsc.li/catalysis

## Hyperconjugation promoted by hydrogen bonding between His98/His241 and a carboxyl group contributes to tyrosine decarboxylase catalysis†

Jie Ni,<sup>a</sup> Guochao Xu,<sup>a</sup> Wei Dai,<sup>a</sup> Yi-Lei Zhao <sup>\*b</sup> and Ye Ni <sup>\*a</sup>

The utility of the  $\sigma \rightarrow \pi^*$  hyperconjugation in pyridoxal 5'-phosphate (PLP)-dependent tyrosine decarboxylase (TyDC) is demonstrated here for the first time. His98 and His241 form hydrogen bonds with the carboxyl group of an external aldimine and contribute to the hyperconjugation of TyDC from *Lactobacillus brevis*. The dihedral angle of C-C $\alpha$ -N<sub>SB</sub>-C4' in PLP-substrate covalent complexes was found to be vital to the decarboxylation efficiency of TyDC.

Pyridoxal 5'-phosphate (PLP, vitamin B6) is widely required as a prosthetic group by many enzymes participating in the metabolism of amines and amino acids.<sup>1,2</sup> Comprehensive research has been conducted on reactions catalyzed by PLP-dependent enzymes throughout the previous decades.<sup>3</sup> A common first step is shared among all PLP-dependent enzyme catalyzed reactions. The aldehyde group of PLP covalently binds to the amino group of highly conserved lysine residues in active sites through an imine bond, forming an internal aldimine. Then, the unprotonated amino group of the substrate attacks the Schiff base of the internal aldimine, breaking the imine bond and forming a new Schiff base between PLP and the amine substrate, which is known as an external aldimine.<sup>4</sup> Afterwards, diverse reaction paths occur according to the specific distribution of key catalytic residues and result in a wide variety of reactions, including transamination, racemization,  $\beta$ -elimination, and retro-aldol cleavage.<sup>5-7</sup>

Nevertheless, the molecular mechanism for the catalytic capacity and divergence in reaction specificity of PLP-dependent enzymes remains largely elusive. A commonly accepted mechanism of the reaction was proposed by

Dunathan *et al.* (1966), in which stereoelectronic effects were important in governing reaction specificity.<sup>8</sup> Their hypothesis for the catalytic mechanism suggests that carboxylate binding sites could modulate the conformations of a C $\alpha$ -N<sub>SB</sub> (SB = Schiff base) bond and the position of residues in the active site. The arrangement of specific residues in active sites would determine which bonds oriented toward C $\alpha$  are likely to be broken. Afterwards, a scissile bond is in an orientation which is parallel to the p orbital of the conjugated  $\pi$  system through hyperconjugation in the external aldimine intermediate.<sup>5</sup> Fundamentally, hyperconjugation is a stabilizing factor for the delocalization of electrons in either bonding  $\sigma$  or  $\pi$  orbitals (HOMO) into an empty or partially occupied antibonding  $\sigma$  or  $\pi$  orbital ( $\sigma^*$  or  $\pi^*$ ) (LUMO).<sup>9</sup> Over 50 years after the original hypothesis, Dajnowicz *et al.* found more detailed physical information connecting the hypothesis and catalytic power employing the neutron structure of recombinant porcine cytosolic aspartate aminotransferase (AAT).<sup>10</sup> In both internal and external aldimines, N1 of PLP was protonated, while O3' of PLP was deprotonated. The substrate in the external aldimine was activated by the AAT enzyme through orienting the C $\alpha$ -H bond perpendicular to the conjugated  $\pi$ -system of PLP and the  $\sigma$  orbital of C $\alpha$ -H parallel to the  $\pi^*$  orbital of the Schiff base, followed by a hyperconjugation effect.<sup>11</sup> In the AAT model, Arg386 and Arg292 form hydrogen bonds with the carboxylate group of the substrate throughout its simulation, which could anchor the substrate in an appropriate conformation for hyperconjugation.<sup>12</sup>

Tyrosine decarboxylase (TyDC, EC 4.1.1.25) is a PLP-dependent fold-type I enzyme<sup>13</sup> that catalyzes the decarboxylation of L-tyrosine, L-3,4-dihydroxy-phenylalanine (DOPA), and other phenolic/indolic amino acids, generating tyramine, dopamine, and corresponding aromatic amines of pharmaceutical relevance.<sup>14,15</sup> TyDC is classified as group II decarboxylase by evolutionary origin, similar to histidine decarboxylase (HDC), glutamate decarboxylase (GDC), and DOPA decarboxylase (DDC).<sup>13</sup> Only two crystal structures of bacterial TyDCs have been resolved and deposited in the protein database:

<sup>a</sup> Key Laboratory of Industrial Biotechnology, Ministry of Education, School of Biotechnology, Jiangnan University, Wuxi 214122, Jiangsu, China.  
E-mail: yni@jiangnan.edu.cn

<sup>b</sup> State Key Laboratory of Microbial Metabolism, Joint International Research Laboratory of Metabolic and Developmental Sciences, MOE-LSB and MOE-LSC, School of Life Sciences and Biotechnology, Shanghai Jiao Tong University, Shanghai 200240, China

† Electronic supplementary information (ESI) available. See DOI: 10.1039/c9cy01290g

one is TyDC from *Methanocaldococcus jannaschii* (PDB code: 3F9T, *Mj*TyDC)<sup>16</sup> and the other is TyDC from *Lactobacillus brevis* (PDB code: 5HSJ, *Lb*TyDC), which was resolved in both *apo* and *holo* structures in our previous study. *Lb*TyDC is a homodimer with an active center located at the interface of dimerization.<sup>17,18</sup> In the *holo* structure of *Lb*TyDC, conserved Lys392 forms an internal aldimine with PLP, while conserved Asp328 directly couples to the pyridinyl nitrogen of PLP.<sup>19,20</sup> Alignment of the crystal structures of *Lb*TyDC and AAT revealed that the spatial arrangement of substrate binding sites is different, which might orient the carboxyl group of tyrosine perpendicular to the PLP conjugated  $\pi$  system in the formation of the external aldimine, leading to the breaking of the C $\alpha$ -COO<sup>-</sup> bond and producing tyramine.<sup>21</sup> The heterolytic cleavage of this C $\alpha$ -C bond is thought to be the rate-limiting step of the decarboxylation reaction catalyzed by TyDC, since this bond is nearly perpendicular to the conjugated  $\pi$ -system of PLP in highly efficient decarboxylases.<sup>22</sup> Besides, studies have demonstrated that ground-state destabilization played a vital role in the catalysis of proton transfer and reaction specificity of some PLP-dependent enzymes.<sup>23,24</sup> To the best of our knowledge, *Lb*TyDC is one of the most efficient tyrosine decarboxylases with a  $k_{\text{cat}}$  of 165 s<sup>-1</sup> as determined by the production of tyramine. Thus, the focus of our study was to explore the key amino acid residues involved in the hyperconjugation in *Lb*TyDC.

The *holo* structure in complex with PLP of *Lb*TyDC was used to generate a model of the external aldimine of *Lb*TyDC.<sup>17</sup> Appropriate substrate conformations were selected for multiple molecular dynamics (MD) simulations. According to the previous QM/MM calculations,<sup>22</sup> the rate-determining step of PLP-dependent decarboxylase was considered to be the decarboxylation step from the external aldimine substrate. The protonation states of the internal and external aldimines are shown in Scheme 1. In accordance with aspartate aminotransferase, the pyridine nitrogen (PLP-N1) was protonated, the phenolic oxygen (PLP-O3') was deprotonated, and the nitrogen of the Schiff base (N<sub>SB</sub>) was protonated in the external aldimine.

Consistent with Dunathan's hypothesis, the density distribution of the dihedral angle of C(C $\alpha$ ), C $\alpha$ , N<sub>SB</sub>, and C4' carbon (C-C $\alpha$ -N<sub>SB</sub>-C4') in the external aldimine of *Lb*TyDC was close to 90° (Fig. 2D), demonstrating that the carboxylate

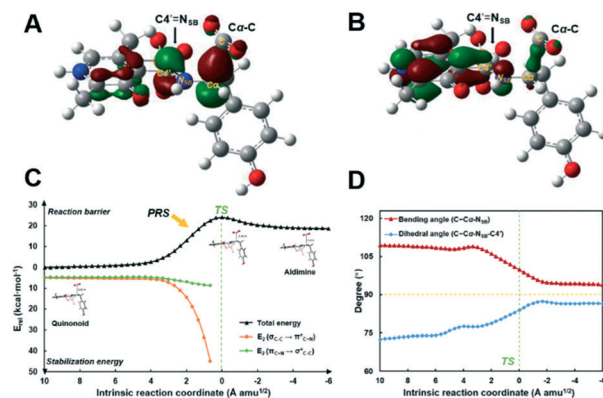


**Fig. 1** Hyperconjugation in TyDC. (A) The highest occupied molecular orbital (HOMO) of the external aldimine structure with stretched C-C bonds in *Lb*TyDC. (B) Lowest unoccupied molecular orbital (LUMO) of the external aldimine structure with stretched C-C bonds in *Lb*TyDC. (C) Reaction potential energy of external aldimine decarboxylation and the stabilization energy of  $\sigma_{\text{C-C}} \rightarrow \pi^*_{\text{N=C}}$  and  $\pi_{\text{N=C}} \rightarrow \sigma^*_{\text{C-C}}$  along the intrinsic reaction coordinate. (D) C-C $\alpha$ -N<sub>SB</sub> bending angle and C-C $\alpha$ -N<sub>SB</sub>-C4' dihedral angle along the intrinsic reaction coordinate.

group was perpendicularly positioned towards the PLP cofactor when using L-tyrosine as a substrate. A cluster analysis was conducted in the equilibrated region of the MD simulations, and Fig. 1 shows the structures with stretched C-C bonds of *Lb*TyDC in complex with the external aldimine from the constrained MD simulations. Considering that the conformation of the external aldimine with the stretched C-C bonds was similar to the transition state, density functional theory (DFT) calculations in combination with HOMO and

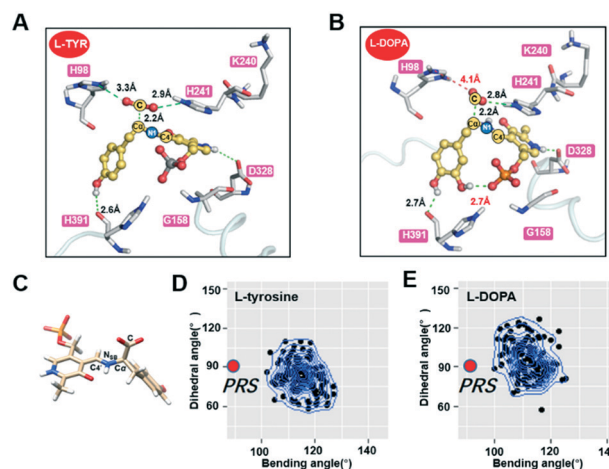
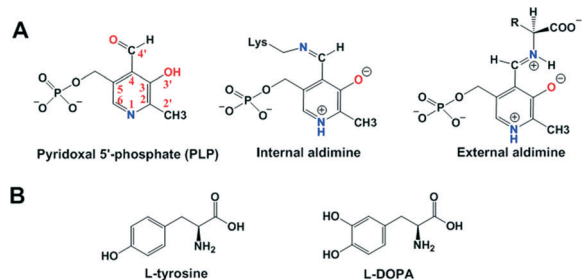


**Fig. 2** Active site of the representative structure and the distribution of the C-C $\alpha$ -N<sub>SB</sub>-C4' dihedral angles in <sup>WT</sup>*Lb*TyDC with L-tyrosine and L-DOPA as the substrate. (A) Active site of <sup>WT</sup>*Lb*TyDC with L-tyrosine in the external aldimine state. (B) Active site of <sup>WT</sup>*Lb*TyDC with L-DOPA in the external aldimine state. Ball and sticks: external aldimine; sticks: key amino acids. (C) External aldimine with labels for atoms included in the torsional angle of interest. (D) Probability density distribution of the C-C $\alpha$ -N<sub>SB</sub>-C4' dihedral angles with L-tyrosine sampled during MD simulations. PRS: best orbital overlapped conformation. (E) Probability density distribution of the C-C $\alpha$ -N<sub>SB</sub>-C4' dihedral angles with L-DOPA sampled during MD simulations.



**Scheme 1** (A) Structures of PLP, internal aldimine, and external aldimine. (B) Structures of L-tyrosine and L-DOPA.

LUMO analysis and natural bond orbital (NBO) analysis were performed on these structures. Comparison of the HOMO and LUMO demonstrated that the charge in the external aldimine was concentrated on the carboxyl group of L-tyrosine and C=N<sub>SB</sub> Schiff base. After the decarboxylation, the negative charge was accommodated on the conjugated  $\pi$ -system of PLP, especially on N<sub>SB</sub>. The second order perturbation theory analysis of the Fock matrix in NBO basis suggested that the donor-acceptor interaction were over 45.0 kcal mol<sup>-1</sup> between  $\sigma$ (C-C $\alpha$ ) and  $\pi^*$ (C=N<sub>SB</sub>) by the  $\omega$ B97x-D(CPCM,water)/6-31G(d) method, respectively (Fig. 1C). This hyperconjugation interaction increased significantly in the pre-reaction state by weakening the C $\alpha$ -C  $\sigma$  bond and provided a substantial contribution to lowering the activation energy. Furthermore, the hyperconjugation effect between C=N<sub>SB</sub> and the breaking C-C $\alpha$  bond was found to be correlated with the bending angle of C-C $\alpha$ -N<sub>SB</sub> and the dihedral angle of C-C $\alpha$ -N<sub>SB</sub>-C4' (Fig. 1D).

The representative conformation with the highest probability was extracted from the MD simulations and analyzed as shown in Fig. 2. Similar to the crystal structure, a number of hydrogen bond interactions exist in the representative conformation of the *LbTyDC* model. Conserved Thr298 and Asp328 form crucial hydrogen bonds with PLP-O3' and PLP-N1, respectively, which were advantageous for the specific protonation states of the PLP cofactor and the optimization of desired chemical transformation. Gly158, Ser159, and Ser440 were responsible for stabilizing the phosphate group of the PLP cofactor. The position of the PLP cofactor was anchored through  $\pi$ - $\pi$  stacking between the imidazole ring of His241 and the pyridine ring of PLP.

Based on the appropriate distance between His98 and L-tyrosine (N $\cdots$ O 3.3 Å) and His241 and L-tyrosine (N $\cdots$ O 2.9 Å), these residues formed hydrogen bonds with the carboxyl group of L-tyrosine during the simulation. These new contacts were the essential interactions between the external aldimine and the active site residues and were responsible for the stabilization of the external aldimine intermediate. These two histidine residues anchored the substrate by orienting the C $\alpha$ -C bond of L-tyrosine perpendicular to the  $\pi$ -conjugated system of the PLP cofactor. The hydrogen bonds between the histidines and the carboxyl group of L-tyrosine positioned the carboxylic group in the correct orientation and this specific orientation leads to the possibility of charge transfer between the occupied and unoccupied orbitals. Interestingly, residues Lys240 and His241 constituted a highly flexible short loop and rotated in response to PLP according to the alignment of *apo-LbTyDC* and *holo-LbTyDC*. When PLP entered the active center of *LbTyDC*, this short loop switched to the opposite position and restrained PLP in the active center. Furthermore, a  $\pi$ - $\pi$  stacking interaction was observed between the pyridine ring of PLP and the imidazole ring of His241, according to the force analysis mentioned above.

To probe the role of key amino acids that contributed to the hyperconjugation in *LbTyDC*, site-directed saturation mutagenesis was performed on His98 (Fig. S2 ESI<sup>†</sup>), Lys240 (Fig.

S3 ESI<sup>†</sup>), and His241 (Fig. S4 ESI<sup>†</sup>). Almost all variants of His241 lost decarboxylase activity toward either L-tyrosine or L-DOPA, and variants H241N, H241S, and H241Q retained less than 5% relative activity of wild-type *LbTyDC* (<sup>WT</sup>*LbTyDC*). The  $k_{\text{cat}}$  toward L-tyrosine of H241N was 4.02 s<sup>-1</sup>, which was only 2.4% of <sup>WT</sup>*LbTyDC* (Table 1). The  $K_{\text{m}}$  values of variants H241S and H241Q significantly increased and could not be precisely determined due to the low solubility of L-tyrosine (5.5 mM). The above results demonstrated that residue His241 played an important role in the decarboxylase activity of *LbTyDC* by: stabilizing the location of the PLP cofactor by  $\pi$ -stacking between the imidazole ring of His241 and the pyridine ring of PLP; orienting the C $\alpha$ -C bond nearly perpendicular to the conjugated  $\pi$ -system of PLP through hydrogen bonding; contributing to the cleavage of the C $\alpha$ -C bond. To explore the role of K240 and H241 on the binding affinity of PLP by *LbTyDC*, the  $K_{\text{D}}$  values toward PLP of <sup>WT</sup>*LbTyDC* and the variants were determined by isothermal titration calorimetry (ITC) (Fig. S5 & Table S1 ESI<sup>†</sup>). <sup>WT</sup>*LbTyDC* exhibited a high affinity toward PLP with a  $K_{\text{D}}$  of  $7.32 \times 10^{-2}$   $\mu\text{M}$ , which was much lower than the  $K_{\text{D}}$  of lysine decarboxylase (72  $\mu\text{M}$ ).<sup>25</sup> The  $K_{\text{D}}$  of H241A increased to  $48.1 \times 10^{-2}$   $\mu\text{M}$ , 6.6-fold higher than that of <sup>WT</sup>*LbTyDC*, whereas H241F has a  $K_{\text{D}}$  value of  $3.81 \times 10^{-2}$   $\mu\text{M}$  (47.7% of <sup>WT</sup>*LbTyDC*). Both the imidazole ring of His241 and the phenyl ring of Phe241 interacted with PLP through  $\pi$ - $\pi$  stacking interactions, while no  $\pi$  system existed in Ala241. It is speculated that the  $\pi$ - $\pi$  stacking interaction was strengthened in Phe241, since the  $K_{\text{D}}$  of H241F was much lower than that of <sup>WT</sup>*LbTyDC*. This further demonstrated the vital role of His241 in PLP binding. The enthalpy change ( $\Delta H$ ) values of <sup>WT</sup>*LbTyDC* and H241F were -5.07 and -5.21 kcal mol<sup>-1</sup> respectively, while the  $\Delta H$  of H241A was -9.06 kcal mol<sup>-1</sup>. Similar binding enthalpies between <sup>WT</sup>*LbTyDC* and H241F indicated that no new hydrogen bond was formed in H241F. However, variants H241A and H241F were almost inactivated towards L-tyrosine and L-DOPA. This result suggests that His241 has dual roles in anchoring PLP and the carboxyl group to form hyperconjugation, and providing its imidazole nitrogen (N $\delta$ 2) as a proton donor in the catalytic reaction. Sequence alignments of tyrosine decarboxylases with more than 40% identities with *LbTyDC* showed that His241 was highly conserved and played an irreplaceable role in the decarboxylation reaction (Fig. S6 ESI<sup>†</sup>).

**Table 1** Kinetic analysis of <sup>WT</sup>*LbTyDC*, H241N and H98M toward L-tyrosine and L-DOPA

Substrate	Variants	Specific activity (U mg <sup>-1</sup> )	$k_{\text{cat}}$ (s <sup>-1</sup> )	$K_{\text{m}}$ (mM)	$k_{\text{cat}}/K_{\text{m}}$ (s <sup>-1</sup> mM <sup>-1</sup> )
L-Tyrosine	WT	43.1 $\pm$ 1.0	165 $\pm$ 2.4	1.18 $\pm$ 0.1	140 $\pm$ 4.1
	H241N	1.35 $\pm$ 0.1	4.02 $\pm$ 0.2	0.05 $\pm$ 0.1	7.28 $\pm$ 0.4
	H98M	1.33 $\pm$ 0.1	4.26 $\pm$ 0.2	0.77 $\pm$ 0.1	5.53 $\pm$ 0.2
L-DOPA	WT	22.5 $\pm$ 1.5	159 $\pm$ 7.7	3.72 $\pm$ 0.3	42.9 $\pm$ 1.5
	H241N	0.08 $\pm$ 0.01	4.02 $\pm$ 0.2	0.05 $\pm$ 0.01	7.28 $\pm$ 0.4
	H98M	1.96 $\pm$ 0.02	7.10 $\pm$ 0.5	1.62 $\pm$ 0.2	4.38 $\pm$ 0.3

Specific activities of the variants of His98 were also determined by saturation mutagenesis. Only H98Q displayed a specific activity of  $23.6 \text{ U mg}^{-1}$ , which is 54% of the activity of  $^{\text{WT}}\text{LbTyDC}$  towards L-tyrosine, while all the other mutants retained less than 10% of the activity of  $^{\text{WT}}\text{LbTyDC}$ . Multiple sequence alignment analyses among various group II decarboxylases revealed that the site with histidine or glutamine was significantly conserved (Fig. S6 ESI†). As mentioned above, His98 formed a hydrogen bond with the carboxyl group of L-tyrosine and restrained it in the hyperconjugative state. When histidine at position 98 was substituted by asparagine, the amide nitrogen of asparagine substituted for the nitrogen of histidine; this also allowed for the formation of a functional hydrogen bond with nitrogen. Significantly, the hydrogen bond between His98 and the carboxyl group of the substrate allowed for an appropriate position for efficient decarboxylation.

It is generally accepted that PLP-dependent group II decarboxylases possess a narrow substrate spectrum and high substrate specificity.<sup>26</sup>  $^{\text{WT}}\text{LbTyDC}$  has lower specific activities of  $26.5 \text{ U mg}^{-1}$  and  $8.36 \text{ U mg}^{-1}$  towards L-DOPA and L-phenylalanine, respectively. L-DOPA was also used as the substrate in the MD simulations. In comparison with L-tyrosine, different conformations were achieved in the MD simulations with L-DOPA due to the extra *m*-hydroxyl group. In a TS-like model, L-DOPA accessed the active center in the form of an electron-hole, and no new hydrogen bonds were formed with other residues. Also, a new hydrogen bond was found between the *m*-hydroxyl of L-DOPA and the phosphate group of PLP, which deformed the external aldimine and weakened the original hydrogen bond between the *p*-hydroxyl of L-tyrosine (Fig. 2). The distance between His98 (N $\delta$ 2) and L-DOPA was 4.1 Å, which is significantly larger than 3.3 Å with L-tyrosine as the substrate.

The dihedral angle of C-C $\alpha$ -N $_{\text{SB}}$ -C4' in the L-DOPA complex became obtuse on the account of the new hydrogen bond between the *m*-hydroxyl of L-DOPA and the phosphate group of PLP. As the dihedral angle increased, the hyperconjugation weakened and a higher activation energy was required to cleave the C-C $\alpha$  bond. The broad distribution of the dihedral angle was predominantly responsible for the lower specific activity toward L-DOPA than L-tyrosine.

Interestingly, H98M showed a higher specific activity toward L-DOPA than L-tyrosine; the specific activities were  $1.96 \text{ U mg}^{-1}$  and  $1.33 \text{ U mg}^{-1}$ , respectively (Table 1). The poor ability of methionine in charge interactions makes it difficult to cleave the C-C $\alpha$  bond. H98M retained low decarboxylase activity. However, the  $k_{\text{cat}}$  of H98M towards L-DOPA was  $7.10 \text{ s}^{-1}$ , which is 66.7% higher than the  $k_{\text{cat}}$  of  $4.26 \text{ s}^{-1}$  towards L-tyrosine. A structural model of H98M was constructed for further MD simulations. When histidine 98 was substituted with methionine, the Dunathan angle of L-tyrosine and the PLP complex became acute, which contributed to the significant reduction in catalytic efficiency. In addition, M98 weakened the distorted conformation of the L-DOPA complex and had a higher specific activity toward L-DOPA than L-tyrosine

(Fig. S7 ESI†). The dihedral angle of C-C $\alpha$ -N $_{\text{SB}}$ -C4' was affected by the interaction between His98 and the carboxyl group of the substrate. The overlapping of the  $\pi$  orbital angles in the transition state was predominantly responsible for the catalytic efficiency.

In conclusion, MD simulations, HOMO and LUMO analysis, NBO analysis, site-directed saturation, and ITC were performed to clarify the key amino acid residues which promoted the hyperconjugation and decarboxylation of LbTyDC. Our results demonstrate that the  $\sigma \rightarrow \pi^*$  hyperconjugation interaction is significant during decarboxylation which can lower the activation energy of the reactants. In LbTyDC, His98 and His241 formed hydrogen bonds with the carboxyl group of the external aldimine and oriented the C $\alpha$ -C bond perpendicular to the conjugated  $\pi$ -system of PLP. These two crucial residues contributed to the  $\sigma \rightarrow \pi^*$  hyperconjugation, and His241 played an irreplaceable role in conformation stability. Besides, the dihedral angle of C-C $\alpha$ -N $_{\text{SB}}$ -C4' in the external aldimine was found to be vital to decarboxylase efficiency and the vertical dihedral angles resulted in the highest breakage efficiency of the C-C $\alpha$  bond.

## Conflicts of interest

There are no conflicts to declare.

## Acknowledgements

This work was supported by the National Key R&D Program (2018YFA0901700, 2018YFA0901200), National Natural Science Foundation of China (21776112, 31770070, 31970041), Natural Science Foundation of Jiangsu Province (BK20171135), National First-Class Discipline Program of Light Industry Technology and Engineering (LITE2018-07), and Top-notch Academic Programs Project of Jiangsu Higher Education Institutions.

## Notes and references

- 1 R. Percudani and A. Peracchi, *BMC Bioinf.*, 2009, **10**, 273.
- 2 P. Christen and P. K. Mehta, *Chem. Rec.*, 2001, **1**, 436–447.
- 3 H. Hayashi, *J. Biochem.*, 1995, **118**, 463–473.
- 4 A. C. Eliot and J. F. Kirsch, *Annu. Rev. Biochem.*, 2004, **73**, 383–415.
- 5 M. D. Toney, *Biochim. Biophys. Acta*, 2011, **1814**, 1407–1418.
- 6 J. P. Richard, T. L. Amyes, J. Crugeiras and A. Rios, *Curr. Opin. Chem. Biol.*, 2009, **13**, 475–483.
- 7 Q. Chen, X. Chen, Y. Cui, J. Ren, W. Lu, J. Feng, Q. Wu and D. Zhu, *Catal. Sci. Technol.*, 2017, **7**, 5964–5973.
- 8 H. C. Dunathan, *Proc. Natl. Acad. Sci. U. S. A.*, 1966, **55**, 712–716.
- 9 I. V. Alabugin, K. M. Gilmore and P. W. Peterson, *Wiley Interdiscip. Rev.: Comput. Mol. Sci.*, 2011, **1**, 109–141.
- 10 S. Dajnowicz, R. C. Johnston, J. M. Parks, M. P. Blakeley, D. A. Keen, K. L. Weiss, O. Gerlits, A. Kovalevsky and T. C. Mueser, *Nat. Commun.*, 2017, **8**, 955.
- 11 S. Dajnowicz, J. M. Parks, X. Hu, R. C. Johnston, A. Y. Kovalevsky and T. C. Mueser, *ACS Catal.*, 2018, **8**, 6733–6737.

- 12 M. D. Toney, *Arch. Biochem. Biophys.*, 2014, **544**, 119–127.
- 13 E. Sandmeier, T. I. Hale and P. Christen, *Eur. J. Biochem.*, 1994, **221**, 997–1002.
- 14 K. Zhang and Y. Ni, *Protein Expression Purif.*, 2014, **94**, 33–39.
- 15 P. J. Facchini and V. De Luca, *Phytochemistry*, 1995, **38**, 1119–1126.
- 16 N. D. Kezmarsky, H. Xu, D. E. Graham and R. H. White, *Biochim. Biophys. Acta, Gen. Subj.*, 2005, **1722**, 175–182.
- 17 H. Zhu, G. Xu, K. Zhang, X. Kong, R. Han, J. Zhou and Y. Ni, *Sci. Rep.*, 2016, **6**, 27779.
- 18 G. Giardina, R. Montioli, S. Gianni, B. Cellini, A. Paiardini, C. B. Voltattorni and F. Cutruzzolà, *Proc. Natl. Acad. Sci. U. S. A.*, 2011, **108**, 20514–20519.
- 19 W. R. Griswold and M. D. Toney, *J. Am. Chem. Soc.*, 2011, **133**, 14823–14830.
- 20 E. F. Oliveira, N. M. Cerqueira, P. A. Fernandes and M. J. Ramos, *J. Am. Chem. Soc.*, 2011, **133**, 15496–15505.
- 21 S. Dajnowicz, J. M. Parks, X. Hu, K. Gesler, A. Y. Kovalevsky and T. C. Mueser, *J. Biol. Chem.*, 2017, **292**, 5970–5980.
- 22 H. S. Fernandes, M. J. Ramos and N. M. Cerqueira, *Chem. – Eur. J.*, 2017, **23**, 9162–9173.
- 23 R. S. Phillips, A. Vita, J. B. Spivey, A. P. Rudloff, M. D. Driscoll and S. Hay, *ACS Catal.*, 2016, **6**, 6770–6779.
- 24 W. R. Griswold, J. N. Castro, A. J. Fisher and M. D. Toney, *J. Am. Chem. Soc.*, 2012, **134**, 8436–8438.
- 25 H. Y. Sagong, H. F. Son, S. Kim, Y. H. Kim, I. K. Kim and K. J. Kim, *PLoS One*, 2016, **11**, e0166667.
- 26 M. P. Torrens-Spence, M. Lazear, R. von Guggenberg, H. Ding and J. Li, *Phytochemistry*, 2014, **106**, 37–43.